RSC Advances

ROYAL SOCIETY OF CHEMISTRY

www.rsc.org/advances

Precursor dissolution temperature as a size-controller in Fe_3O_4 submicrospheres synthesis and their effect in catalytic degradation of Rhodamine B

Beatriz da Costa Carvalho[a], Fabiana Cristina Andrade Corbi[a], Fernando Aparecido Sigoli[a] and Italo Odone Mazali[a,*]

[a] *Functional Materials Laboratory – Institute of Chemistry – University of Campinas - UNICAMP, P.O. Box 6154, Zip Code 13083-970 - Campinas - SP- Brazil*

* Author to whom correspondence should be addressed.
E-mail: mazali@iqm.unicamp.br
Phone: +55 19 35213164 / Fax: +55 19 35213023

Abstract

Iron oxides submicrospheres have been synthesized by solvothermal method. Particle sizes decrease from 700 to 100 nm as a function of dissolution temperature of iron salt precursors, keeping constant the reaction temperature in the autoclave. The submicrospheres particles are formed by aggregation of smaller nanoparticles, nanograins. Fe_3O_4 submicrospheres show high saturation magnetization (M_s) and low hysteresis (low remnant magnetization, M_r and coercivity, H_c), showing superparamagnetic behavior. The size tailoring of the iron oxide particles allowed their application as catalyst on photo-Fenton reaction of Rhodamine B degradation, in which smaller particles showed high catalytic activity and the degradation efficiency showed strong dependence on the nanograin size.

***Keywords*:**

Iron oxide, solvothermal synthesis, dissolution of iron salt precursor, temperature effect, Rhodamine

Introduction

The synthesis of magnetic iron oxide particles has been widely explored in the last decades due to their potential application as catalysts, chemical sensors, theranostic materials in biological systems, etc[1,2,3,4]. These magnetic nanoparticles show interesting properties such as high saturation magnetization and superparamagnetic behavior, i.e., the magnetic response of the particles is immediately canceled by removing the external magnetic field, and thus, they can be easily used in catalysis and biomedical application[5] The magnetic properties may be adjusted in accordance with the methodology of the particles preparation. Several chemical methods can be used to prepare magnetic iron oxide particles such as co-precipitation[6], microemulsions[7], sonochemical[8], hydrothermal[9] and solvothermal[10] reactions and thermal decomposition[11], which can provide nano/micro particles of magnetite (Fe_3O_4) with controlled size and morphology. In general, such particles must provide high chemical stability, uniform size distribution and facile dispersion in aqueous medium. In this study the solvothermal method was chosen because it produces highly dispersed particles and narrow size distribution. The reaction consists in dissolving a precursor of Fe^{III} and a precipitating agent, such as sodium acetate in a particular solvent which must also promotes the reduction of ions Fe^{III} to Fe^{II} such as ethylene glycol, to obtain $(Fe^{II})(Fe^{III})_2O_4$ with inverted spinel structure. In some cases surfactants are also used to stabilize the particles in the process of magnetite formation at high pressure, such as polyvinylpyrrolidone (PVP), polyethylene glycol (PEG).

It has been observed that the variation of different parameters in the solvothermal synthesis may affect directly the morphology and size of nanoparticles. Fan et al.[12] studied the Fe^{III} concentration effect on particle sized and observed that the particle size increases as a function of the precursor concentration. Shen et al.[13] used

diethylene glycol as solvent and reducing agent, and sodium citrate as growth inhibitor to obtain nanoparticles from 2 to 13 nm highly stable in water ("water-soluble"). Zhu and Diao[14] investigated the influence of different parameters of the reaction such as the concentration of precursor and precipitant agent, reaction time and autoclave temperature on the morphology and size of the particles. They observed that an increase in autoclave temperature leads to smaller particles size. When the concentrations of the precipitant agent or Fe^{III} precursors were low, porous nanospheres with small size were obtained. The authors observed that the autoclave reaction time directly affects the final magnetic properties of the products. However, to the best of our knowledge, the effect of dissolution temperature of iron salt precursor in the properties of iron oxides was not investigated.

In our previous study, we showed that maghemite nanoparticles synthesized in a Vycor® glass exhibit typical superparamagnetic behaviors[15]. In the present study, we report the solvothermal synthesis of iron oxide particles using ethylene glycol as the solvent and reducing agent, while sodium acetate and polyethylene glycol were used as precipitating and stabilizing agents, respectively. The influence of dissolution temperature of iron salt precursor in ethylene glycol was evaluated according of magnetic behavior, crystal phase, morphology and particles size. Furthermore, the degradation of Rhodamine B under visible light, using H_2O_2 as the oxidation reagent in a photo-Fenton reaction was chosen as a model reaction to investigate the effect of particle size on the catalytic activity of the Fe_3O_4

Experimental section

Materials

All chemicals were analytical grade and used as received. $FeCl_3$ and Rhodamine B (RhB) were purchased from Sigma-Aldrich, $CH_3COONa·3H_2O$ (NaAc), ethylene glycol (EG) and polyethylene glycol 4000 (PEG) from Vetec, Hydrogen peroxide (H_2O_2, 30%) from Synth.

Synthesis of Fe_3O_4 particles with different particle size

Fe_3O_4 particles were prepared via solvothermal synthesis[16]. Typically, 5.0 mmol of $FeCl_3$ were dissolved in 40 mL of EG, followed by addition of 26.5 mmol of NaAc and PEG (1.0 g). The mixture was stirred vigorously for 30 min at room temperature to form a homogeneous solution. In order to evaluate the effect of dissolution temperature of iron salt precursors (before autoclave step) on morphology and particle size, the mixture solution was heated at different temperatures (25, 40, 60, 80, 100, 120 and 140 °C), and then transferred and sealed in a Teflon-lined stainless-steel autoclave (80 mL of capacity). The autoclave was heated to 200 °C for 8 h to complete the reaction. The products were collected and rinsed several times with deionized water and ethanol, then dried under vacuum at 60 °C for 15 h.

Catalytic Activity of Fe_3O_4 in heterogeneous photo-Fenton degradation of RhB

The photocatalytic activities of the Fe_3O_4 particles were evaluated by photo-Fenton degradation of RhB with H_2O_2 under UV-Vis irradiation (125 W Hg lamp with a 399 nm cut-off filter). For RhB degradation, 12 mg of Fe_3O_4 was suspended in 10 mL of a 1.0×10^{-5} mol L^{-1} RhB aqueous solution. Before irradiation, the RhB-catalyst suspension was dispersed in the dark for 5 min. 1.24 mmol of H_2O_2 was added to the solution at the beginning of the irradiation. The concentration of RhB at different

reaction times was determined by UV spectroscopy (Varian Cary-50 spectrophotometer).

Characterization

X-ray powder diffraction (XRD) was performed on Shimadzu XRD-7000 diffractometer, operating with CuKα radiation (λ = 1.5406 Å, 40 kV, 30 mA). Infrared spectra (FTIR) were obtained on a Bomem MB100 Spectrometer using a KBr pellet with resolution of 4 cm^{-1}. The morphology and particle size were determined by Scanning Electron Microscopy (SEM) in a FEI Inspect-50 microscope and Transmission Electron Microscopy (TEM) in a HR-TEM JEOL 3010 (300 kV) equipment from the National Nanotechnology Laboratory (LNNano). The magnetic behavior of the samples was investigated by the Vibrating Sample Magnetometer technique (VSM) on a LakeShore-7400 magnetometer with a maximum magnetic field equal to 2.0 Tesla. The measurements were performed at room temperature.

Results and Discussion

Iron oxide particles using classical solvothermal synthesis: precursor dissolution at room temperature

The classical solvothermal synthesis was performed to be used as a reference. The diffraction peaks were indexed (Figure 1a) and magnetite phase was identified (Fe_3O_4, JCPDS 19-0629). The crystallite size (D) was evaluated by Debye-Scherrer equation[17] ($D=k\lambda/\beta\cos\theta$), where k is a shape constant (equal to 0.9 assuming that the crystallite is spherical), λ is the X-ray wavelength (1.5406 Å), θ is the Bragg diffraction

angle (deg.), and β is the full-width at half-maximum (rad.) of the diffraction peak (311) with higher intensity. To this sample, the crystallite size was calculated as 77 nm.

The FTIR spectrum (Figure 1b) shows a single band at 583 cm^{-1} assigned to ν(FeO) in magnetite. In addition, other two bands are observed with lower intensity ascribed to $\delta(CH_2)$ at 1431 cm^{-1} and ν(COC) at 1076 cm^{-1}. These bands indicate the presence of a small amount of PEG in the sample.

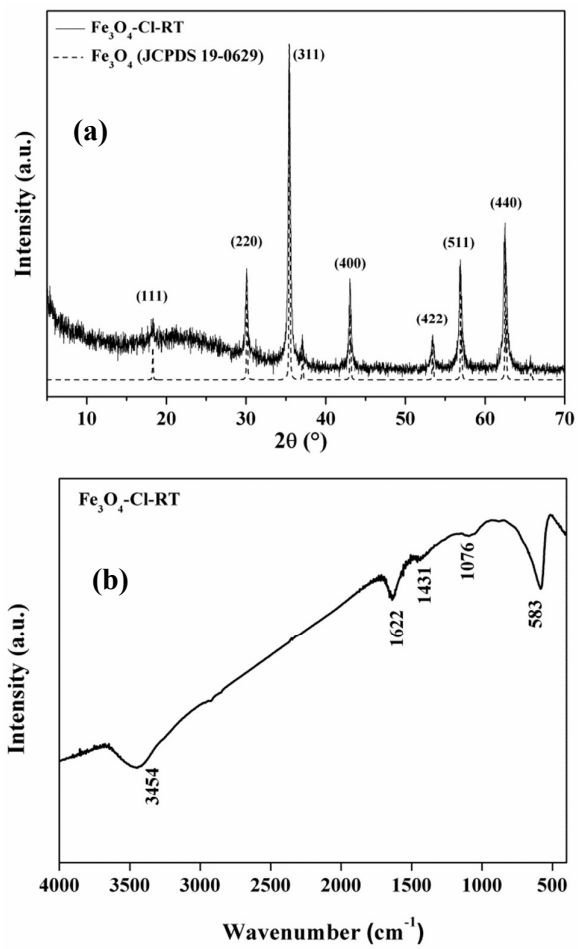

Figure 1. (a) XRD and **(b)** FTIR of the Fe_3O_4-Cl-RT sample

The morphology of the particles obtained with precursors dissolution at room temperature was investigated by SEM, the images are shown in Figure 2. The particles are spheroidal with particle size of ca. 700 nm. The particles surface is rough, as can be

clearly seen in the Figure 2c. The microsphere particles are formed by aggregation of smaller nanograins (Figure 2c).

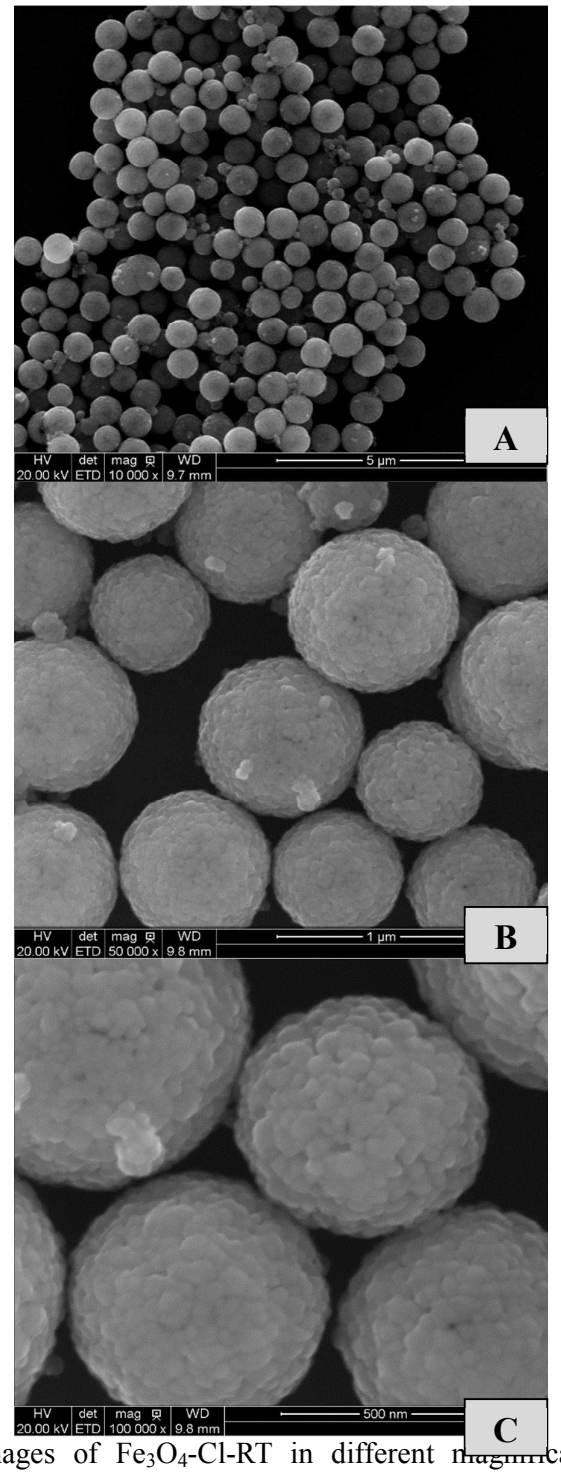

Figure 2. SEM images of Fe_3O_4-Cl-RT in different magnifications revealing the nanograins structures

Based on the results obtained from the magnetite particles here synthesized and on the literature[18,19,20,21], two steps to obtain these particles are proposed. Firstly, in the precursors dissolution $FeCl_3$, EG, NaAc and PEG (before autoclave step), the formation of iron(III) acetate is observed (reddish precipitate). In the second step, which occurs in the autoclave at high temperature and pressure, the partial reduction of Fe^{III} to Fe^{II} by EG occurs, leading to the formation of the respective Fe^{II} and Fe^{III} hydroxides, which lead to the magnetite phase. Therefore, in this paper a new strategy of particle size control was used by changing the temperature of precursors dissolution before the solvothermal reaction.

Dissolution temperature of precursors before solvothermal process: size, morphology, crystal structure and magnetic properties of Fe_3O_4

Usually, the procedure of salt dissolution is carried out at room temperature, but in this study the dissolution temperature was raised from 40 to 140 °C, keeping the other synthesis conditions unchanged, as shown in Scheme 1.

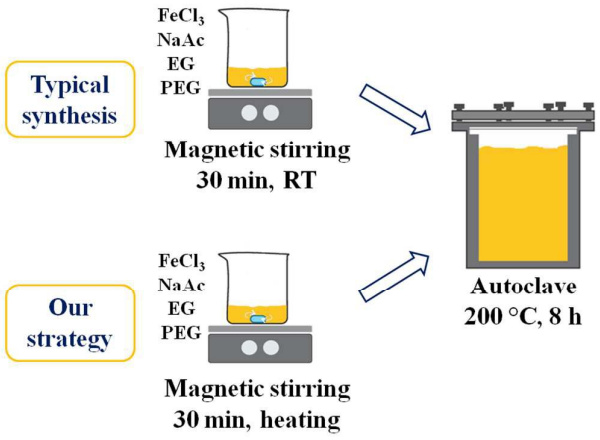

Scheme 1. Experimental arrangement of the Fe_3O_4 synthesis, highlighting the step of dissolution of iron salt precursors under heating. The autoclave temperature was kept at 200 °C for all experiments, and the change was carried out just in the step of $FeCl_3$, NaAc, EG and PEG mixture before autoclave process.

The XRD pattern of the samples shown in Figure 3 reveals that all diffraction peaks may be indexed to magnetite (Fe_3O_4 JCPDS 19-0629). It can be noticed that the peaks broaden as the dissolution temperature increases, indicating the formation of smaller crystals. The crystallite size was calculated by Debye-Scherrer equation and one may observe (Table 1) that their size decreases as the dissolution temperature increases SEM images show that the nanograins are equivalent to crystallite size, as can be seen in Figure 4. Particles with 700 nm formed by aggregation of 77 nm grains were obtained when the precursors dissolution was carried out at room temperature, while at 140 °C the particle size is c.a.100 nm with nanograins of c.a. 13 nm. Therefore, as the dissolution temperature increases, the nanograin and particles sizes decrease. These results reveal that the dissolution temperature plays an important role on controlling the Fe_3O_4 particle sizes obtained by solvothermal process.

Table 1. Parameters of Fe_3O_4 microspheres prepared using different temperatures of dissolution of precursors.

Sample	Temperature dissolution of precursors / °C	Particle size / nm[a]	Crystallite size / nm[b]	Mr / emu g^{-1}	Hc / Oe
Fe_3O_4-Cl-RT	25	700	77	7.2	51.8
Fe_3O_4-Cl-40	40	700	77	6.8	60.5
Fe_3O_4-Cl-60	60	600	78	6.3	67.5
Fe_3O_4-Cl-80	80	350	70	7.6	65.4
Fe_3O_4-Cl-100	100	150	28	5.5	33.2
Fe_3O_4-Cl-120	120	115	20	3.7	23.0
Fe_3O_4-Cl-140	140	100	13	1.9	9.5

[a]Measured by SEM, [b]Measured by XRD

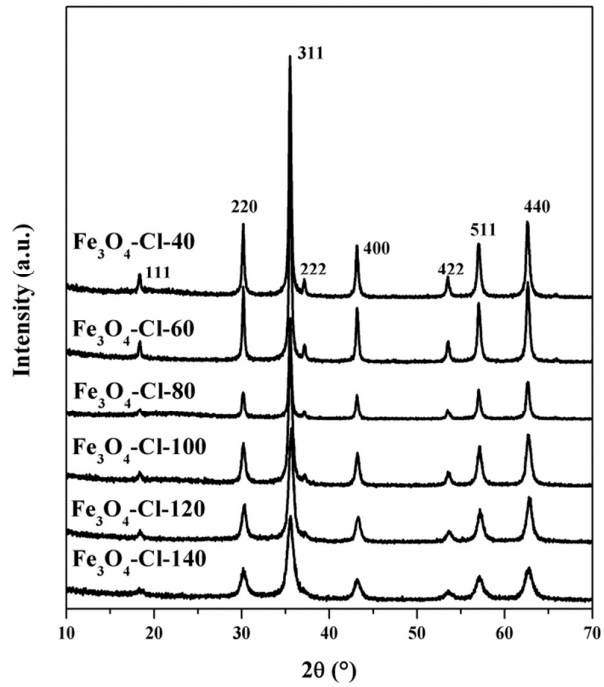

Figure 3. XRD pattern of **Fe_3O_4-Cl-T** (T= 40-140 °C) samples

Some studies have showed that the initial concentration of precursors affects the formation of nanocrystals and consequently the size of microspheres[14,20]. In the present study, it was noticed for the first time that the precursor dissolution temperature plays direct influence on the particle and their crystallite sizes. It is known that the formation of Fe_3O_4 includes nucleation of the oxide, followed by the growth of these nuclei to form primary crystals (nanograins) which will organize to form larger submicrospheres[14]. Some authors have shown that the particle size decreases as the water content decreases due decrease the ratio ethylene glycol/water (EG/W)[20,22]. It is possible that evaporation of water during heating causes lower EG/W ratio explaining the small size for particles whose synthesis was carried out in high temperature dissolution of precursors. However, the procedure performed in reflux condenser does not show change on particle size, such fact confirms the temperature influence has main role in the particle size.

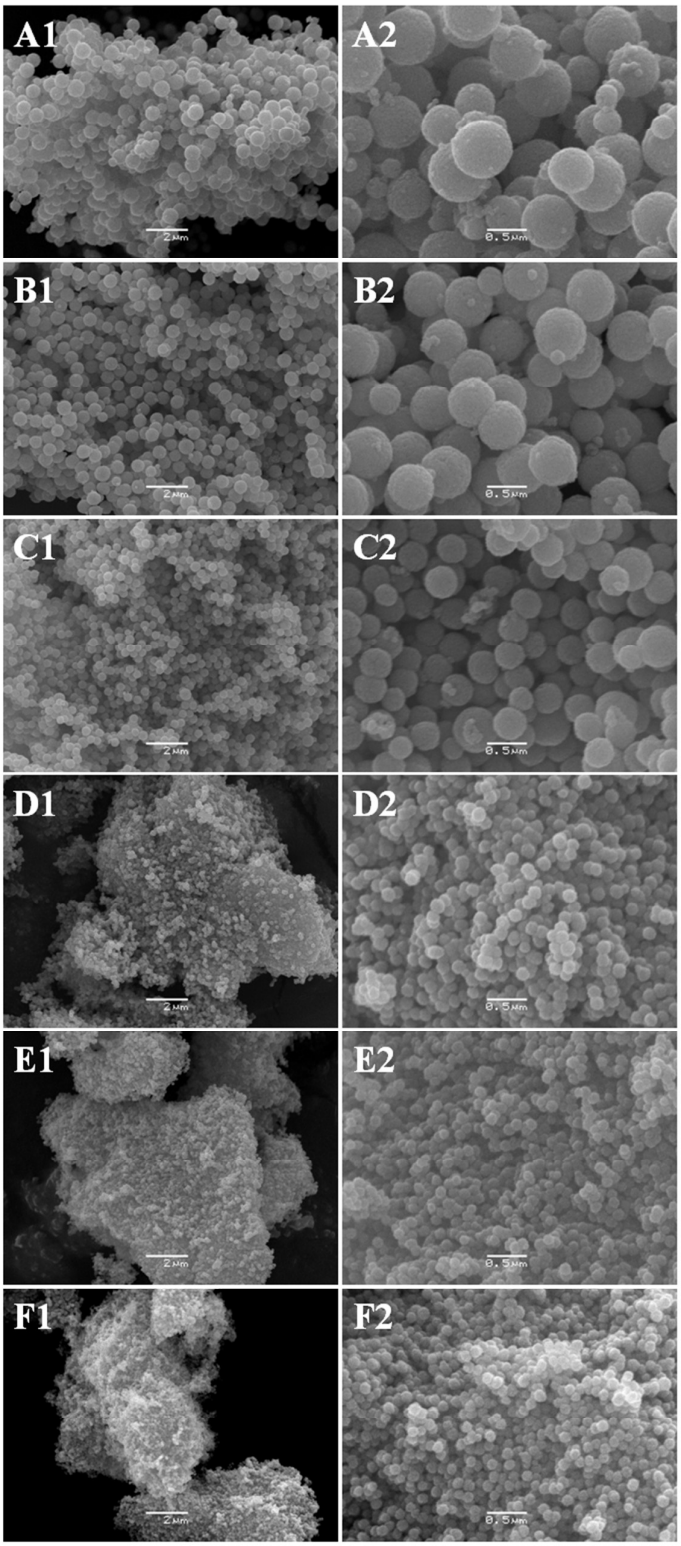

Figure 4. SEM images of the Fe_3O_4 synthesized in different precursor dissolution temperature. **A**: 40 °C, **B**: 60 °C, **C**: 80 °C, **D**: 100 °C, **E**: 120 °C, **F**: 140 °C. On the left column the bar is 2 μm. On the right column the bar is 0.5 μm for all samples.

The morphology and size of the particles were investigated by SEM. Figure 4 shows SEM images of the Fe_3O_4 microspheres synthesized at different precursor dissolution temperatures. One may clearly see that the higher the dissolution temperature the smaller the particle size. The particle size of the sample Fe_3O_4-Cl-40 and Fe_3O_4-Cl-60 (Figure 4c and 4b) do not show significant changes compared to the sample obtained at room temperature Fe_3O_4-Cl-RT (Figure 2). The Fe_3O_4-Cl-80 sample (Figure 4c) has an average particle size of 350 nm, that is about the half of the magnetite particle size obtained at room temperature (classic synthesis[16]). When the precursor temperature dissolution is 100 °C, 120 °C and 140 °C (Figure 4d, 4e and 4f), the mean sizes of particles are 150 nm, 115 and 100 nm, respectively, and they are about seven times smaller than those obtained by classical synthesis.

TEM images also show that the particles are also formed by nanograins similar to those obtained by classical synthesis. (see detail in Figure 5). The Fe_3O_4 particle is made of aggregates of nanograins and therefore may be understood as a nanostructured particle. Spheroidal particles of c.a. 700 nm are formed by nanograins of 60 nm, while those with diameter of 150 nm are formed by nanograins of 15 nm, implying that the precursor temperature dissolution has a direct influence on nanograin size and consequently on the final particle size.

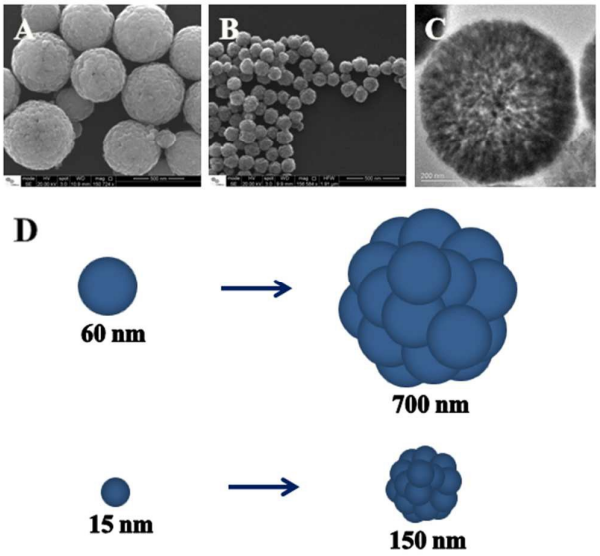

Figure 5. SEM high magnification of the Fe_3O_4 microspheres (**A**: Fe_3O_4-Cl-40, **B**: Fe_3O_4-Cl-100), (**C**): TEM of the Fe_3O_4-Cl-40 and (**D**): scheme of the formation of Fe_3O_4 nanostructure with different size formed from nanograins, demonstrating that smaller grains grow in smaller particles

The FTIR spectra of all Fe_3O_4 samples show a band at 583 cm^{-1} corresponding to the Fe-O lattice mode of Fe_3O_4 (Figure 6). The other signals observed in the spectra indicate the presence of a small amount of PEG or EG in the samples.

The magnetic properties of the microspheres were evaluated using a vibrating sample magnetometer (VSM), measured at room temperature. The magnetic measurements of Fe_3O_4-Cl-RT sample (magnetite obtained with reaction mixture at room temperature) show magnetization saturation (M_s), remanent magnetization (M_r) and coercivity (H_c) values of 85 emu g^{-1}, 7.2 emu g^{-1} and 51.8 Oe, respectively. The hysteresis loops shown in Figure 7 suggests the superparamagnetic behavior of the sample. Furthermore, these spheres with homogeneous dispersion showed fast response to the external magnetic field due to its superparamagnetic properties.

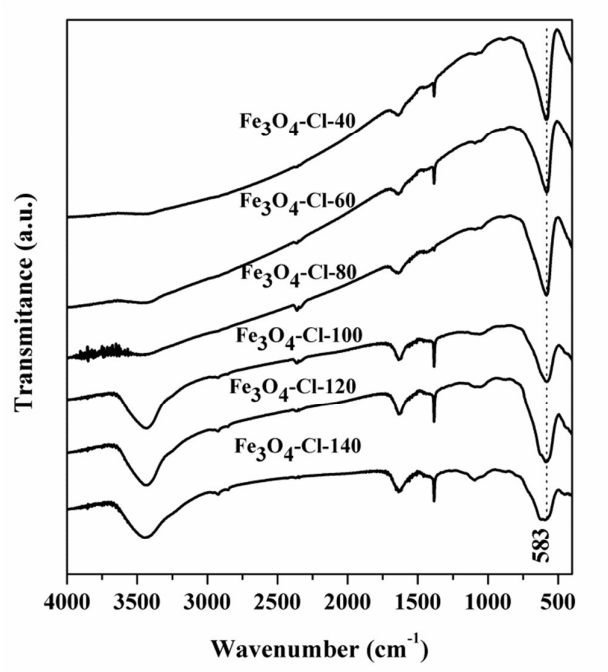

Figure 6. FTIR spectra of the Fe_3O_4 samples at different precursors dissolution temperatures

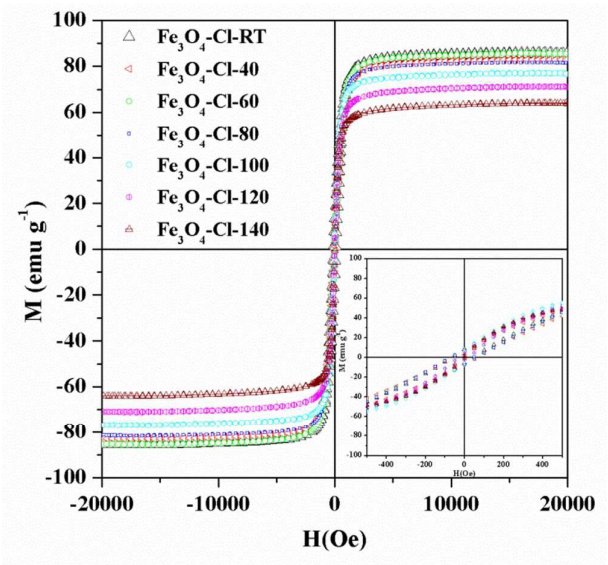

Figure 7. Magnetic hysteresis loops of Fe_3O_4 at different temperature of precursors dissolution

All samples obtained from the modified precursor dissolution temperature show the same magnetization profile curve (Figure 7). The data showed in Table 1 indicate that the M_s decrease while the particle size decreases

The decrease in M_s is due to higher contribution of surface effects, anisotropy and non-stoichiometry of smaller diameters particles. Because of the spin disorder on the particles surface, such particles tend to have lower M_s than the respective bulk. The spin disorder is directly related to the magnetic behavior of the system[23,24,25]. M_r and H_c of the samples also decreased as the particle size decreases (Table 1), and it is known that superparamgnetic particles do not exhibit M_r and H_c, being very interesting in biomedical and catalytic applications due to null residual magnetization observed after magnetic field removal. 700 nm magnetic particles show H_c 60.5 Oe and M_r 6.8 emu g^{-1} values, being lower than reported by Fan et al[12] in nanostructured particles with 130 nm. The smaller particles (100 nm) obtained in this work show the H_c = 9.5 and M_r = 1.9. Thus, it can be seen that the values of H_c and H_r tend to zero as the particle sizes decreases. The magnetic properties of the particles with size above critical diameter to Fe_3O_4 superparamagnetic (ca. 60 nm)[26] can be explained due to nanograin size that aggregate to form a submicrosphere (100 to 700 nm) thus the superparamgnetic response, low coercivity and magnetization remanent can be assigned to the nanograins.

Catalytic Activity of the Fe_3O_4 particles with different sizes

The Fe_3O_4 particles with different sizes can be used in heterogeneous catalytic degradation of organic compounds. The photo-Fenton reaction was used as model reaction to study the catalytic properties of these magnetic particles. RhB was chosen as organic dye to degradation reaction by H_2O_2 under UV-Vis radiation. The UV-Vis degradation curves are presented on Figure S1 (Supporting Information). As shown in

Figure 8a, without Fe_3O_4 particles, the degradation is very low (less than 5%, considered negligible), being attributed to the low oxidation potential of H_2O_2 as compared to hydroxyl radicals (OH)[27]. When Fe_3O_4-Cl-140 was irradiated under visible radiation without H_2O_2 (Figure 8b), it was observed a little RhB degradation, approximately 10%, due to adsorption of RhB in Fe_3O_4 catalyst. The effect of the particles size in degradation efficiency was evaluated using 100, 350 and 700 nm Fe_3O_4 particles.

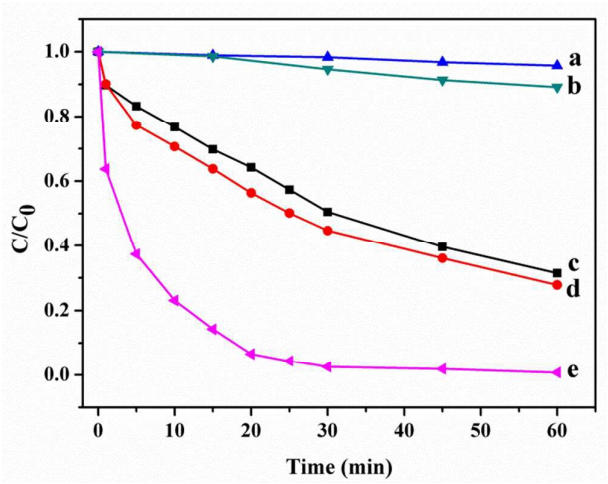

Figure 8. Degradation of RhB under different conditions: (a) RhB/H_2O_2/vis; (b) RhB/Fe_3O_4-Cl-140/vis; (c) RhB/ Fe_3O_4-Cl-RT/ H_2O_2/vis; (d) RhB/ Fe_3O_4-Cl-80/ H_2O_2/vis; (e) RhB/ Fe_3O_4-Cl-140/ H_2O_2/vis

The RhB degradation of the 700 and 350 nm particles (Figure 10c and 10d, respectively) is similar, around 70% in 60 min. Although these particles have different sizes, there is almost no difference in their crystallite size (nanograin), as can be seen in Table 1, being about 77 nm (Fe_3O_4-Cl-RT) and 70 nm (Fe_3O_4-Cl-80), and thus this slight difference is not enough to promote higher catalytic activity for the 350 nm microspheres. However, the degradation of RhB by H_2O_2 using 100 nm magnetite

particles (Fe_3O_4-Cl-140) under Vis irradiation reached 100% in 60 min (Figure 8e), showing higher efficiency for RhB degradation. The smaller crystallite size (13 nm) contributes to enhance the catalytic effect in these particles for RhB degradation probably because the higher surface/volume ratio. Furthermore, the catalysts can be conveniently separated by applying an external magnetic field.

Conclusions

Fe_3O_4 nanostructured spheroidal particles have been obtained by modified solvothermal method. The synthesis leads to nanostructured spheres formed by nanograins that aggregate to form submicroparticles. The dissolution of iron precursor at different temperatures before autoclave process provided a control of the particle size without changing the morphology. As the precursor dissolution temperature increases, the particle size decreases, being possible to obtain particles from 100 to 700 nm formed by different nanograins sizes. The particles showed superparamagnetic properties, high magnetization saturation and small M_r and H_c. The precursor dissolution temperature is an important synthesis parameter that can be changed to modulate the size of particles depending on the need of the application. Fe_3O_4 particles showed to be highly efficient in RhB degradation by photo-Fenton reaction, demonstrating the influence of crystallite size on catalytic activity of the particles, with best results for 100 nm particles and 13 nm crystallite.

Acknowledgements

The authors would like to thank the FAPESP, CAPES and CNPq agencies for financial supports. Contributions from Brazilian Nanotechnology National Laboratory (LNNano, Campinas-SP) for SEM and TEM are also gratefully acknowledged. This is a

contribution of the National Institute of Science and Technology in Complex Functional Materials (CNPq-MCT/FAPESP).

References

1. E. Andronescu, M. Ficai, G. Voicu, D. Ficai, M. Maganu and A. Ficai, *Journal of Materials Science: Materials in Medicine*, 2010, **21**, 2237-2242.
2. G.-D. Fang, D. D. Dionysiou, S. R. Al-Abed and D.-M. Zhou, *Applied Catalysis B: Environmental*, 2013, **129**, 325-332.
3. A. Ito, H. Honda and T. Kobayashi, *Cancer Immunology, Immunotherapy*, 2006, **55**, 320-328.
4. H. Qiu, C. Luo, M. Sun, F. Lu, L. Fan and X. Li, *Carbon*, 2012, **50**, 4052-4060.
5. M. Mahmoudi, S. Sant, B. Wang, S. Laurent and T. Sen, *Advanced Drug Delivery Reviews*, 2010, **63**, 24-46.
6. W. Zhang, S. Jia, Q. Wu, J. Ran, S. Wu and Y. Liu, *Materials Letters*, 2011, **65**, 1973-1975.
7. P. A. Dresco, V. S. Zaitsev, R. J. Gambino and B. Chu, *Langmuir*, 1999, **15**, 1945-1951.
8. F. Dang, N. Enomoto, J. Hojo and K. Enpuku, *Ultrasonics Sonochemistry*, 2009, **16**, 649-654.
9. T. J. Daou, G. Pourroy, S. Bégin-Colin, J. M. Grenèche, C. Ulhaq-Bouillet, P. Legaré, P. Bernhardt, C. Leuvrey and G. Rogez, *Chemistry of Materials*, 2006, **18**, 4399-4404.
10. A. Yan, X. Liu, G. Qiu, H. Wu, R. Yi, N. Zhang and J. Xu, *Journal of Alloys and Compounds*, 2008, **458**, 487-491.

11. D. Maity, P. Chandrasekharan, P. Pradhan, K.-H. Chuang, J.-M. Xue, S.-S. Feng and J. Ding, *Journal of Materials Chemistry*, 2011, **21**, 14717-14724.
12. T. Fan, D. Pan and H. Zhang, *Industrial & Engineering Chemistry Research*, 2011, **50**, 9009-9018.
13. L.-h. Shen, J.-f. Bao, D. Wang, Y.-x. Wang, Z.-w. Chen, L. Ren, X. Zhou, X.-b. Ke, M. Chen and A.-q. Yang, *Nanoscale*, 2013, **5**, 2133-2141.
14. M. Zhu and G. Diao, *The Journal of Physical Chemistry C*, 2011, **115**, 18923-18934.
15. D. Cangussu, W. C. Nunes, H. L. d. S. Corrêa, W. A. d. A. Macedo, M. Knobel, O. L. Alves, A. G. S. Filho and I. O. Mazali, *Journal of Applied Physics*, 2009, **105**, 013901.
16. P. Yang, Z. Quan, Z. Hou, C. Li, X. Kang, Z. Cheng and J. Lin, *Biomaterials*, 2009, **30**, 4786-4795.
17. R. Jenkins and R. L. Snyder, *Introduction to x-ray powder diffractometry*, John Wiley & Sons, New-York, 1996.
18. Q. Q. Xiong, J. P. Tu, Y. Lu, J. Chen, Y. X. Yu, Y. Q. Qiao, X. L. Wang and C. D. Gu, *The Journal of Physical Chemistry C*, 2012, **116**, 6495-6502.
19. S. Liu, R. Xing, F. Lu, R. K. Rana and J.-J. Zhu, *The Journal of Physical Chemistry C*, 2009, **113**, 21042-21047.
20. M. Jean, V. Nachbaur and J.-M. Le Breton, *Journal of Alloys and Compounds*, 2012, **513**, 425-429.
21. L.-L. Wang and J.-S. Jiang, *Nanoscale Research Letters*, 2009, **4**, 1439-1446.
22. S.-B. Cho, J.-S. Noh, S.-J. Park, D.-Y. Lim and S.-H. Choi, *Journal of Materials Science*, 2007, **42**, 4877-4886.

23. B. D. Cullity, C. D. Graham, *Introduction to magnetic materials,* John Wiley, Hoboken, 2009.
24. A. Yan, X. Liu, G. Qiu, H. Wu, R. Yi, N. Zhang and J. Xu, *Journal of Alloys and Compounds*, 2008, **458**, 487-491.
25. O. Moscoso-Londono, D. Muraca, L. A. S. de Oliveira, K. R. Pirota and L. M. Socolovsky, *Magnetics, IEEE Transactions on*, 2013, **49**, 4551-4554.
26. S. Mörup, M. F. Hansen and C. Frandsen, in *Comprehensive Nanoscience and Technology*, Academic Press, Amsterdam, Editon edn., 2010, pp. 437-491.
27. S. Guo, G. Zhang and J. Wang, *Journal of Colloid and Interface Science*, 2014, **433**, 1-8.